

Original Research Paper

Reduction of Radiation Effects in Biomedical Imaging Detectors by Technology Change

¹Essesse Songa Auguste, ¹Wembe Tafo Evariste, ²Madinatou Salomon and ³Belinga Aboudou Jean

¹Department of Physics, Faculty of Science, University of Douala, B.O. Box, 24157 Douala, Cameroon

²Department of Physics, Faculty of Science, University of Yaoundé I, B.O. Box 812 Yaoundé, Cameroon

³Department Electrical Engineering, ENSET, University of Douala, B.O. Box, 24157 Douala, Cameroon

Article history

Received: 19-05-2021

Revised: 09-06-2021

Accepted: 10-06-2021

Corresponding Author:

Wembe Tafo Evariste
Department of physics, Faculty
of science, University of
Douala, B.O. Box, 24157
Douala, Cameroon
Email: twembee@yahoo.fr

Abstract: Silicon is a preferred material in the design of medical imaging detectors. It enables reliable and inexpensive detectors to be produced. However, the operation of this material is compromised when irradiated with high radiation of more than 5×10^{14} particles/cm² of high energy neutrons. The defects caused transform the electrical properties. Therefore, this loss of information compromises the reconstruction of important events. This research paper aims to make a scientific contribution to the reduction of this radiation effects. The proposed solution is obtained by changing the silicon material generally used to design the detectors by a carbon nanotube material. The use of carbon nanotube material allows the detector to reduce the effects of radiation and leakage currents. A particular observation was made on the linear attenuation coefficient μ , the radiation length X_0 and the width of the forbidden band E_g . Our results show the best characteristics for a carbon nanotube material compared to silicon. For a cross thermal section equal to $\sigma_{Si} = \sigma_c = 2 \times 10^{-3}b$, the carbon linear attenuation coefficient is greater than the silicon ($\mu_{Si} = 9.979 \times 10^{-5} \text{cm}^{-1} < \mu_C = 3.533 \times 10^{-4} \text{cm}^{-1}$). For a maximum effective cross section of equal diffusion $\sigma_C = 1009 \times 10^{-3}b$, ($\mu_{Si} = 0.503 \times 10^{-3} \text{cm}^{-1} < \mu_C = 1.732 \times 10^{-3} \text{cm}^{-1}$), for a minimum effective cross section of equal diffusion $\sigma_{Si} = \sigma_C = 10.09 \times 10^{-3}b$, $\mu_{Si} = 0.503 \times 10^{-3} \text{cm}^{-1} < \mu_C = 1.732 \times 10^{-3} \text{cm}^{-1}$. $X_{0_{Si}} = 22.009 \text{ g/cm}^2$ and $X_{0_C} = 42.969 \text{ g/cm}^2$, $E_{g_{Si}} = 1.2 \text{ e.V}$ and $E_{g_{Si}} = 5.5 \text{ e.V}$. From these results, the carbon material has an attenuation coefficient at least three times higher than that of the silicon material.

Keywords: Silicon, Carbon, Technology Change, Radiation, Biomedical Imaging, Attenuation Coefficient, Material

Introduction

With the progress of microelectronics, we are witnessing the improvement of the living conditions of human beings in several areas such as communication, transport, medicine (Lanzarotti, 1990; Bulletin, 1985; Lemoine, 2015) etc. This is why man is always in search of well-being in the face of the difficulties encountered. It is in the same order, for example, that Research programs in particle physics, nuclear physics, astrophysics and medicine are growing in number (Evariste *et al.*, 2010). In biomedical imaging, most of the detectors used are made from silicon semiconductors on a microscopic scale (Davia, 2003). However, the radiations resulting from the collision between the electromagnetic radiation and the matter very often affect the detector by its effects of

radiations (Wunstorf, 1997; Claeys and Simoen, 2002). This subsequently leads to the deterioration of the sensors, thus modifying the information of the expected results. However, by virtue of its properties, diamond being essentially made up of carbon, we find that the latter is an excellent resistant to radiation (Besson, 2015; Bortolamiol, 2015). For this purpose, we propose in this article, the change of the silicon material generally used by a carbon nanotube material. According to the research of Chantepie (2008; Besson, 2015), it emerges that a good detector is chosen according to the thickness of the substrate, the width of the forbidden band, the density of the material. Despite the wealth of recent research on the characteristics of a good detector, no paper has noted the change in technology from silicon material to carbon nanotube material. Therefore, our study focused on an

analytical and numerical analysis of the characteristics of carbon nanotubes. This article is structured as follows, firstly, we will do an analytical and comparative study where we will compare the attenuation coefficient, the length of radiation and band gap width of silicon material relative to carbon nanotube material. Then the continuation, one will make a numerical study in which we seek the variations of the coefficients of these two materials according to the thermal effective section and maximum and minimum cross sections of diffusion. To better understand our work, the results obtained and the interpretation of these results will be the subject of our attention in turn. At the end, we will make a conclusion.

Analytical and Comparative Study

A study has shown that two effects of radiation damage detectors when exposed to electromagnetic radiation (Wunstorf, 1997; Claeys and Simoen, 2002). As we said above, this study is based on the analysis and comparison of three determining parameters for the choice of a good detector exposed to electromagnetic radiation. We will begin our study with the linear attenuation coefficient of a material given by formula (Chantepie, 2008):

$$\mu = N_A \frac{\rho}{A} \sigma (cm^{-1}) \tag{2}$$

where, μ is the linear attenuation coefficient, ρ is the density of the material, N_A is the Avogadro constant and σ is the cross section and A is the molar mass of the material.

Then, the coefficients of silicon and carbon are respectively given by:

$$\mu_{Si} = \rho_{Si} \frac{N_A}{A_{Si}} \sigma_{Si} (cm^{-1}) \tag{2}$$

$$\mu_c = \rho_c \frac{N_A}{A_c} \sigma_c (cm^{-1}) \tag{3}$$

By differentiating these coefficients, we obtain the following expression:

$$\mu_c - \mu_{Si} = N_A \left(\sigma_c \frac{\rho_c}{A_c} - \sigma_{Si} \frac{\rho_{Si}}{A_{Si}} \right) \tag{4}$$

and the simplest case, with equal section this expression becomes:

$$\mu_c - \mu_{Si} = N_A \sigma \left(\frac{\rho_c}{A_c} - \frac{\rho_{Si}}{A_{Si}} \right) (cm^{-1}) \tag{5}$$

where the values of the constants ρ_c and ρ_{Si} are taken from the Table 1 (Chantepie, 2008; Besson, 2015).

Another determining parameter for the choice of a good detector is the length of radiation noted X_0 , which is actually a physical quantity of choice of a material relating to the loss of energy by electromagnetic interaction (Isabelle, 2009)

The expression for this length is given by (Eidelman, 2004):

$$X_0 = \frac{716.4 \times A}{Z(Z+1) \ln \frac{287}{\sqrt{Z}}} (g/cm^2) \tag{6}$$

where, A and Z are the molar mass and atomic number of the material, respectively.

Then, the radiation lengths of silicon and carbon are respectively given by:

$$X_{0_{Si}} = \frac{716.4 \times A_{Si}}{Z_{Si}(Z_{Si}+1) \ln \frac{287}{\sqrt{Z_{Si}}}} (g/cm^2) \tag{7}$$

$$X_{0_c} = \frac{716.4 \times A_c}{Z_c(Z_c+1) \ln \frac{287}{\sqrt{Z_c}}} (g/cm^2) \tag{8}$$

and by differentiating these two lengths $X_{0_c} - X_{0_{Si}}$, we get the expression:

$$716,4 \left(\frac{A_c}{z_c(z_c+1) \ln \frac{287}{\sqrt{z_c}}} - \frac{A_{Si}}{z_{Si}(z_{Si}+1) \ln \frac{287}{\sqrt{z_{Si}}}} \right) \tag{9}$$

In addition, it should be noted that the choice of the material to be used will be that which has the greatest length of radiation. The choice of a detector also depends on the band gap E_g , the larger this width the considerably good and the leakage current considerably decreases (Chantepie, 2008). By observing the Table 1, we can easily note this width and make the difference between the width of the forbidden band of the material with the carbon nanotube and that of silicon.

Digital Study

For this study, we will approach three cases of figures. In the first, given that we are in the high frequencies, we will work with the thermal cross section, the order of magnitude of which varies between $2 \times 10^{-27} cm^2$ and $3.4 \times 10^{-27} cm^2$. With equal cross section of carbon and silicon, we collected the data in Table 2. These data will allow us to simulate on MATLAB, the variations of the attenuation coefficients of carbon and silicon as a function of the cross section. The second and third

numerical study relate respectively to the reading of the attenuation coefficients maximum and minimum cross sections of diffusion the data of which are recorded on Table 3 and 4 (Thiollière, 2005).

Presentation of the Results

Table1 (Chantepie, 2008; Besson, 2015) shows the characteristics of some semiconductors. These characteristics permitted us to determine the values of the densities and the widths of the forbidden bands of the materials.

With an equal cross section, the difference $\mu_C - \mu_{Si}$ of Eq. (5) is equal to $2.5351 \cdot 10^{-1} \text{ cm}^{-1}$. The ratio between the attenuation coefficients of carbon and silicon determined

$$\text{is } \frac{\mu_C}{\mu_{Si}} \cong 3.54 .$$

On the other hand, the radiation lengths of silicon and carbon are respectively:

$$\begin{cases} X_{0Si} = 22.009 \text{ g / cm}^2 \\ X_{0C} = 42.969 \text{ g / cm}^2 \end{cases}$$

The difference and the ratio between the two radiation lengths gives us respectively:

$$\begin{cases} X_{0C} - X_{0Si} = 20.96 \text{ g / cm}^2 \\ \text{and} \\ \frac{X_{0C}}{X_{0Si}} = 1.952337 \end{cases}$$

Moreover, using Table 1 for the widths of the forbidden bands, we note that:

$$\begin{cases} E_{gSi} = 1.2e.V. \\ \text{and} \\ E_{gC} = 5.5e.V. \end{cases}$$

Table 1: Inventory of the main characteristics of materials used for particle detection

Material	Z	Density g/cm ⁻³	E _g eV	E _p eV	μ _n Cm ² /Vs	τ _e ⁻ s	μ _p cm ² / (Vs)	τ _p ⁺ s
Si	14.0	2.32	1.12	3.60	1450	1.10 ⁻³	450	2.10 ⁻³
Ge	32.0	5.33	0.67	2.96	3900	1.10 ⁻³	1900	1.10 ⁻³
AsGa	32.0	5.32	1.43	4.30	8000	10.10 ⁻⁹	400	100.10 ⁻⁷
CdTe	50.0	5.85	1.52	4.43	1100	3.10 ⁻⁶	100	2.10 ⁻⁶
Cd _{0,9} Zn _{0,1} Te	49.1	5.78	1.57	4.64	1000	3.10 ⁻⁶	80	1.10 ⁻⁶
diamond	6.0	3.52	5.50	13.00	1800	10 ⁻³	1200	< 10 ⁻³
a-Si	14.0	2.30	1.80	4.00	1	7.10 ⁻⁹	5.10 ⁻³	4.10 ⁻⁶
a-Se	34.0	4.30	2.20	7.00	5.10 ⁻³	1.10 ⁻⁶	1.4 10 ⁻¹	1.10 ⁻⁶
HgI ₂	62.0	6.40	2.13	4.20	100	1.10 ⁻⁶	4	1.10 ⁻⁵
PbI ₂	62.7	6.20	2.32	4.90	8		2	

Table 2: Statement of the attenuation coefficients of silicon and carbon materials as a function of the cross section

σ(cm ²)×10 ⁻²⁷	2	2.1	2.2	2.3	2.4	2.5	2.6
μ _C (cm ⁻¹)×10 ⁻⁶	353.3	370.965	388.63	406.295	423.96	441.625	459.29
μ _{Si} (cm ⁻¹)×10 ⁻⁶	99.796	104.7858	109.7756	114.7654	119.7552	124.745	129.7348
σ(cm ²)×10 ⁻²⁷	2.7	2.8	2.9	3	3.1	3.2	3.3 3.4
μ _C (cm ⁻¹)×10 ⁻⁶	476.955	494.62	512.285	529.95	547.615	565.28	582.945 600.61
μ _{Si} (cm ⁻¹)×10 ⁻⁶	134.7246	139.7144	144.7042	149.694	154.6838	159.6736	164.6634 169.6532

Table 3: Statement of the attenuation coefficients of silicon and carbon materials as a function of the maximum cross section of diffusion

σ(cm ²)×10 ⁻²⁵	9.830	9.790	9.74	9.86	10.09	9.810	9.780	9.840	10.08
μ _C (cm ⁻¹)×10 ⁻³	1.735	1.728	1.719	1.741	1.781	1.732	1.727	1.737	1.779
μ _{Si} (cm ⁻¹)×10 ⁻³	0.490	0.488	0.485	0.491	0.503	0.489	0.487	0.490	0.502

Table 4: statement of the attenuation coefficients of silicon and carbon materials as a function of the minimum cross section of diffusion

σ(cm ²)×10 ⁻²⁵	9.230	9.390	9.340	9.220	9.650	9.250	9.740	9.240	9.360
μ _C (cm ⁻¹)×10 ⁻³	1.629	1.658	1.649	1.628	1.704	1.633	1.659	1.631	1.705
μ _{Si} (cm ⁻¹)×10 ⁻³	0.460	0.468	0.465	0.459	0.481	0.461	0.468	0.460	0.481

The difference and the ration between the forbidden bandwidths give us respectively:

$$\left\{ \begin{array}{l} E_{gC} - E_{gSi} = 4.3eV. \\ \text{and} \\ \frac{E_{gC}}{E_{gSi}} = 4.9107 \end{array} \right.$$

For the numerical study, with an equal thermal cross section and variable between $2 \times 10^{-27} \text{ cm}^2$ and 3.4×10^{-27} and. We have recorded the values of attenuation coefficients of silicon and carbon materials as a function of the cross section in Table 2 (Bauer *et al.*, 1998).

By also making the ratio of the means between the carbon and silicon attenuation coefficient for Table 2, 3 and 4, we find respectively:

$$\frac{\mu_{C2}}{\mu_{Si2}} = 3.540, \frac{\mu_{C3}}{\mu_{Si3}} = 3.548 \text{ and } \frac{\mu_{C4}}{\mu_{Si4}} = 3.544$$

Interpretation of Results

The analytical study allowed us notice that:

$$\left\{ \begin{array}{l} \mu_C - \mu_{Si} > 0 \\ X_{0C} - X_{0Si} > 0 \text{ and } \\ E_{gC} - E_{gSi} > 0 \end{array} \right. \left\{ \begin{array}{l} \frac{\mu_C}{\mu_{Si}} > 1 \\ \frac{X_{0C}}{X_{0Si}} > 1 \\ \frac{E_{gC}}{E_{gSi}} > 1 \end{array} \right.$$

According to these results for this study, we find that the carbon nanotube material has a better attenuation coefficient $\left(\mu_C - \mu_{Si} > 0 \text{ and } \frac{\mu_C}{\mu_{Si}} > 1 \right)$, has a greater radiation length and a greater band gap compared to the silicon material. We can therefore say that the carbon material biomedical imaging detector will better reduce the effects of radiation and leakage currents compared to silicon material.

Numerically, the Fig. 1, 2 and 3 below, showing the curves of the attenuation coefficients of carbon nanotube materials and silicon. We notice that in these three cases, the curves of the attenuation coefficients of carbon radiation are always above those of silicon whatever the nature of the nature of the effective section. On the other hand, we find that the attenuation coefficient of the carbon nanotube material increases with the cross section for Fig. 1 but, with a few exceptions, can even reach a peak following a certain value of the effective section. At the same time for Fig. 1, the attenuation coefficient of silicon material first decreases and then increases slightly with the cross section. For Fig. 2 and 3, the variation in the attenuation coefficient of the carbon and silicon material varies very little as a function of the effective section. All these remarks lead us to say that with a few exceptions, the attenuation coefficient of a material increases the effective section of the latter. Therefore, the greater the cross section of the material, the more the detector can considerably reduce the effects of radiation. The maximum value of the radiation attenuation coefficient of the carbon material is reached when the effective section of the latter takes the value $28 \times 10^{-27} \text{ cm}^2$.

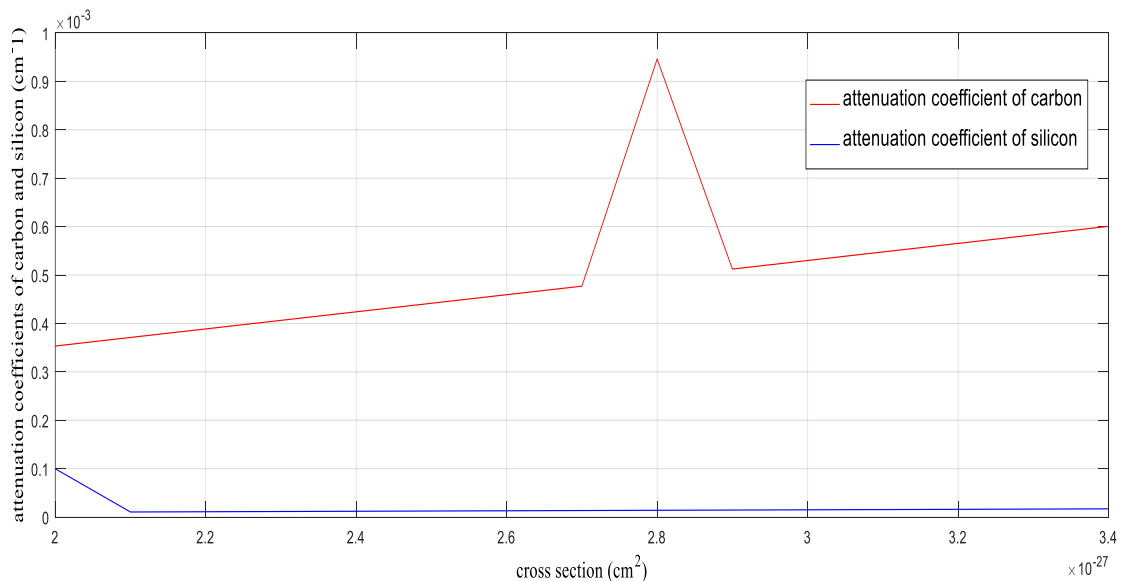


Fig. 1: Curves of the attenuation coefficients of carbon and silicon as a function of the thermal cross section

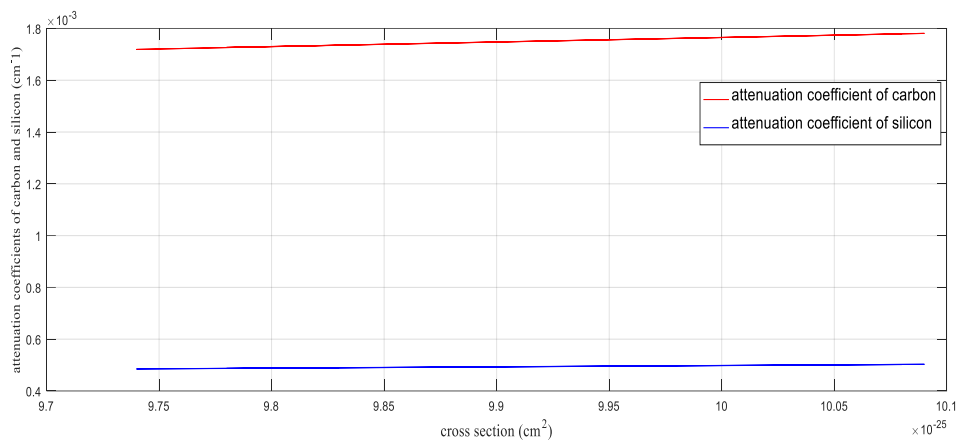


Fig. 2: Curves of the variations of the attenuation coefficient of silicon and carbon materials as a function of the maximum cross section of diffusion

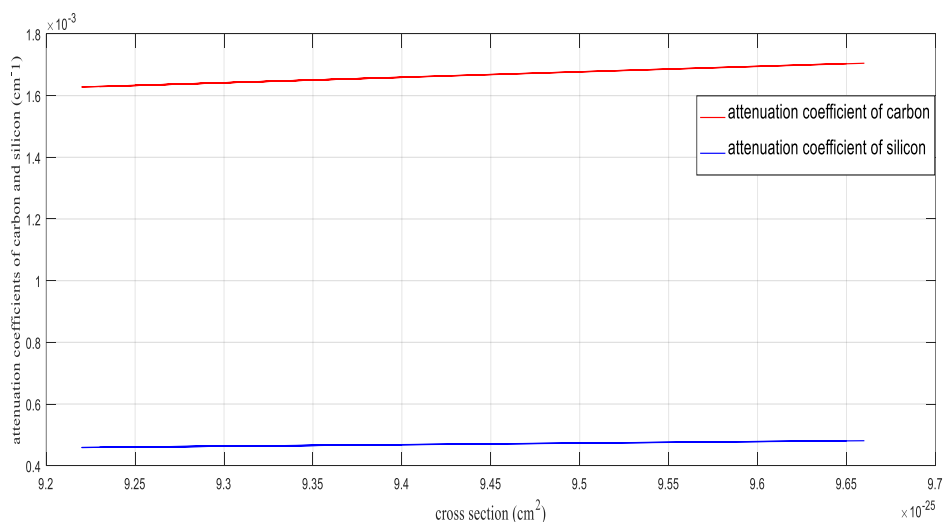


Fig. 3: Curves of the variations of the attenuation coefficient of silicon and carbon materials as a function of the minimum cross section of diffusion

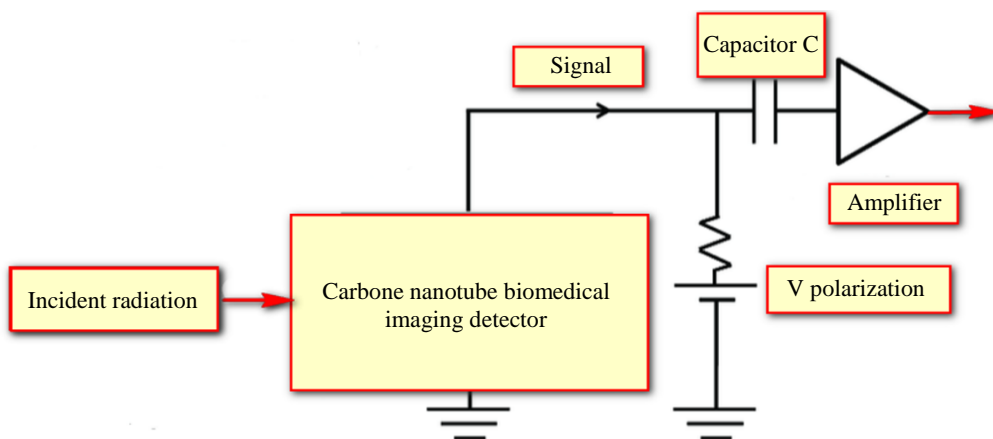


Fig. 4: diagram of the biomedical imaging detection device

Presentation of the Carbon Nanotube Biomedical Imaging Detector

In a simplified way, here is the functional diagram of the detection device (Legou, 2002) this diagram is a representation of the general operating principle of the detection chain by semiconductor detectors in imaging, see Fig. 4. This principle can be summed up in four steps. The first step is materialized by the interaction of incident radiation in the active material of the detector. This interaction is accompanied by a partial deposition of the energy of the incident radiation on the one hand, but also by the creation of charge carriers (electron/ion pairs) on the other hand. The second stage is marked by the transport, the collection of a signal and the measurement of an induced current linked to the movement of these charge carriers created in the first stage (Knoll and Wiley, 1989). The third step is marked by the processing and amplification of the signal delivered by the detector by an electronic circuit (Lemoine, 2015). In other words, this part is reserved for the reduction of the disturbances which accompany the signal to a certain extent but also the amplification of the latter (Foulquier and Radiol, 2010). The last step marked by the transfer of the signal to a data acquisition and storage system for use.

Conclusion

At the end of our research, the aim of which was to propose one of the solutions to reduce the effects of radiation on the biomedical imaging detector. We recall that the main goal is to reduce the effects of radiation on the detection device. On the other hand, it was also a question of reducing the leakage currents. The results obtained show that the ratio between the attenuation coefficients of carbon and silicon $\left(\frac{\mu_c}{\mu_{Si}}\right)$ is approximately equal to 3.5. In the same perspective, the ratio between the forbidden bandwidths $\left(\frac{E_{gC}}{E_{gSi}}\right)$ give us 4.9107. In other words, the carbon material is at least three and a half times more resistant to radiation than the silicon material on the one hand. On the other hand, the carbon material can significantly reduce the leakage currents five times compared to the silicon material. In view of all observations, we can say that carbon nanotubes are more resistant to the effects of radiation compared to silicon material on the one hand. On the other hand, because of the large value of band gap, carbon nanotubes reduce leakage currents that can affect the system. It is therefore possible to reduce not only the effects of radiation on the imaging detector, but also to considerably reduce the leakage currents which can disturb the information

expected when using the carbon material. We can say that carbon nanotube is near future and reliable solutions for biomedical imaging. For the moment, the limits of our work lie on experimentation. This is why, in a near future, we would like to work on themes such as: Experimental study of data from carbon and silicon detector intended for medical imaging. General study of materials to determine the best medical imaging detector and where possible, design the best imaging detector.

Author's Contributions

Esesse Songa Auguste: Performed some of the experiments through simulation software.

Wembe Tafo Evariste: Project leader, data interpretation and contribute to writing of the paper.

Madinatou Salomon and Belinga Aboudou Jean: Contribute to the writing of the paper.

Ethics

The corresponding author confirms that all of the other authors have read and approved the manuscript and no ethical issues involved.

References

- Bauer, R. W., Anderson, J. D., Grimes, S. M., Knapp, D. A., & Madsen, V. A. (1998). Application of a simple Ramsauer model for neutron total cross sections. *Nuclear science and engineering*, 130(3), 348-360. <https://www.tandfonline.com/doi/abs/10.13182/NSE98-A2011>
- Besson, A. (2015). Détecteurs à semi-conducteur conducteurs, juin 2015.
- Bortolamiol, T. (2015). Nanotubes de carbone biparois: fonctionnalisation et détection in vitro (Doctoral dissertation). <https://oatao.univ-toulouse.fr/13943/>
- Bulletin, A. (1985). Microelectronics based automation technologies and development, n°2 Novembre 1985, Centre for science and technology development, united Nations New-york
- Chantepie, B. (2008). Study and realization of fast low noise electronics for a hybrid pixel X-ray detector intended for small animal imaging (Doctoral dissertation, Université de la Méditerranée-Aix-Marseille II). <https://tel.archives-ouvertes.fr/tel-00366861/>
- Claeys, C., & Simoen, E. (2002). Radiation effects in advanced semiconductor materials and devices (Vol. 57). Springer Science & Business Media. ISBN-10: 3540433937.
- Davia, C. (2003). Détecteurs au silicium radiorésistants: une solution d'avenir » université Brunei, Royaume-Uni, 2003.

- Eidelman, S. (2004). Review of particle physics. Particle Data Group. 2004.
- Evariste, W. T., Hong, S., Q., Jie, K., & Tongxi, W. A. N. G. (2010). Design and simulation of Gaussian shaping amplifier made only with CMOS FET for FEE of particle detector, Nuclear Science and Techniques Vol.21, No 5, October 2010 P.312-315
- Foulquier, J. N. and Radiol, J. (2010). Technical parameters to decrease the radiation dose from conventional and digital radiographs. 2010.
- Knoll, G. F., & Wiley, E. D. (1989). Radiation detection a measurement., 1989. ISBN-10 : 0470131489
- Lanzarotti, M. (1990). Micro-electronic automation: challenges for the Third World. Third World Review, 285-309. <https://www.jstor.org/stable/23591503>
- Legou, T. (2002). Etude et réalisation d'une chaîne d'instrumentation numérique rapide pour l'identification des ions (Doctoral dissertation, Université de Caen). <https://tel.archives-ouvertes.fr/tel-00002517/>
- Lemoine, T. (2015). Imagerie médicale par rayons X- Caractérisation des détecteurs de rayons X. <https://www.techniques-ingenieur.fr/base-documentaire/biomedical-pharma-th15/imagerie-medicale-42607210/imagerie-medicale-par-rayons-x-med202/>
- Thiollière, N. (2005). Mesure des sections efficaces de diffusion élastique des neutrons sur le carbone et le fluor dans le domaine épithermique sur la plate-forme PEREN (Doctoral dissertation, Université Joseph-Fourier-Grenoble I). <https://tel.archives-ouvertes.fr/tel-00011285/>
- Isabelle, W. (2009). Les Détecteurs en physique des particules, 2009.
- Wunstorf, R. (1997). Radiation hardness of silicon detectors: current status. IEEE Transactions on Nuclear Science, 44(3), 806-814. <https://ieeexplore.ieee.org/abstract/document/603757/>